Modeling and Control of a Piezo-Actuated High-Dynamic Compensation Mechanism for Industrial Robots

Björn Olofsson, Olof Sörnmo, Ulrich Schneider, Anders Robertsson, Arnold Puzik and Rolf Johansson

***Abstract*— This paper presents a method for modeling and control of a piezo-actuated high-dynamic compensation mechanism (HDCM) for usage together with an industrial robot during a machining operation, such as milling in aluminum. The spindle is attached to the compensation mechanism and the robot holds the workpiece. Due to the inherent resonant character of mechanical constructions of this type, and the nonlinear phenomena appearing in piezo actuators, control of the compensation mechanism is a challenging problem. This paper presents models of the construction, experimentally identified using subspace-based identification methods. A subsequent control scheme, based on the identified models, utilizing state feedback for controlling the position of the spindle is outlined. Experimental results performed on a prototype of the HDCM are also provided.**

I. Introduction

Due to the limited positioning accuracy and stiffness of industrial robots, machining has traditionally been performed using dedicated CNC machines, when accuracy less than 0.1 mm is required. However, since industrial robots may offer more flexible and cost efficient machining solutions than CNC machines, it is desirable to use industrial robots for machining tasks, such as, *e.g.*, milling in aluminum.

Within the EU/FP7-project COMET [1], the aim is to develop solutions for machining with industrial robots with accuracy below 50 μm. For high-precision machining, a high-dynamic mechanism for real-time compensation of the remaining position errors of the robot is developed. This unit is called a High-Dynamic Compensation Mechanism (HDCM).

This paper presents modeling and control of a prototype of the HDCM-unit. The construction of the unit has been discussed in several papers before, see, *e.g.*, [2], [3], and therefore, the mechanical design is only briefly described below. The focus of this paper will be on the dynamic properties and how the subsequent control design should be optimized for satisfactory milling results. It will be shown how nonlinear effects in the HDCM can be handled and how the mechanical vibrations in the construction can be reduced by using appropriate control design methods.

This paper is organized as follows. Section II describes the experimental setup of the industrial robot and the HDCM-unit, as well as the corresponding environment for simulation and testing of the control design. Section III describes initial experiments performed on the HDCM for dynamic characterization. Based on the dynamic characterization, modeling of the construction is discussed in Section IV and the subsequent model-based control design is described in Section V. Experimental results are presented in Section VI and finally conclusions and future work are given in Section VII.

B. Olofsson, O. Sörnmo, A. Robertsson and R. Johansson are with the Department of Automatic Control, LTH, Lund University, SE–221 00 Lund, Sweden. E–mail: Bjorn.Olofsson@control.lth.se.

U. Schneider and A. Puzik are with Fraunhofer Institute for Manufacturing and Engineering, Nobelstrasse 12, D-70569 Stuttgart, Germany.

Fig. 1. The experimental setup for real-time compensation of positioning errors during machining operations, where the robot holds the workpiece and the spindle holding the milling tool is mounted on the HDCM-unit.

II. Experimental setup

A prototype of the HDCM has been developed at Fraunhofer IPA in Stuttgart, Germany, where the unit is located. In the experiments, the HDCM is to be used together with a REIS RV40 industrial robot. The robot holds the workpiece and the spindle is consequently attached to the HDCM, see Fig. 1.

A. Construction

The construction of the HDCM is such that motion of the spindle is possible in three Cartesian directions, hereafter called x, y and z, respectively. The three axes are designed to be decoupled. The motion in each direction is achieved by the forces generated by three individual piezo actuators. The extensions of the piezo actuators are translated to a corresponding translational movement of the spindle *via* a flexure mechanism. The flexure mechanism is constructed such that the gear ratio of the displacement of the spindle and the extension of the piezo actuator is approximately five in each direction.

B. Actuation and sensors

The extension of the piezo actuators is changed by applying a voltage, and the extensions are measured using strain gauges, attached to the actuators. The Cartesian displacement of the spindle is measured with capacitive sensors, one in each direction.

C. Interface to the HDCM

In order to develop the control structure for the HDCM-unit, all sensors and actuators are integrated using a dSPACE system of model DS1103 [4]. Using the software ControlDesk, the user can implement new control strategies in a simple manner as well as develop graphical user interfaces. The control design described in this paper has been implemented in MATLAB Simulink, then generated to C–code using the *Real-Time Workshop* toolbox [5]. The compiled C-code is installed in the dSPACE system and executed at a sampling frequency of 10 kHz.

III. Dynamic characterization of the construction

Due to the inherent resonant character of mechanical systems and the nonlinear effects that appear in piezo actuators, accurate positioning control of the HDCM without vibrations is a challenging control problem. A model-based solution is here pursued in order to control the tool position.

A. Nonlinear phenomena in the piezo actuators

Experiments have been performed on the HDCM in order to determine the effect of the nonlinear phenomena in the piezo actuators. The experiments indicated that the main nonlinearities that need to be handled are hysteresis and the creep phenomenon. Results from experiments where the voltage to the piezo actuators are alternatingly increasing and decreasing are shown in Figs. 2–3. From the results displayed in these figures it is obvious that the hysteresis needs to be handled actively for accurate positioning. It is also noted that the hysteresis is both rate and amplitude dependent. On the other hand, experiments showed that the nonlinear creep phenomenon in the actuator is a much slower process, and thus easier to handle.

Although different in nature, both of these nonlinear effects can be handled using high-gain feedback. The control design will be described in Section V.

B. Frequency characterization of the mechanical construction

In order to characterize the frequency properties of the mechanical construction, several frequency response experiments have been performed. The frequency spectra in the different directions, displayed in Fig. 4, were estimated using the periodogram method. An important property of the system is the location of the first natural eigenfrequency. It is noted that the characteristics are quite different in the three Cartesian directions. In particular, two natural eigenfrequencies are visible in the x- and z-axes, whereas only one is visible in the y-direction. The first eigenfrequency

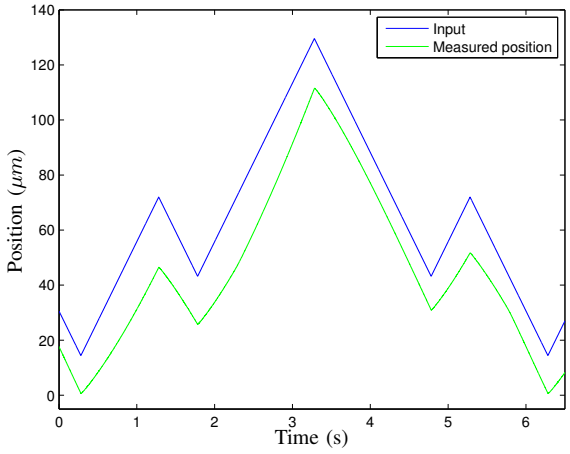

Fig. 2. Experiment where a triangular wave with varying amplitude is applied as input to the piezo actuator. The hysteretic behavior is clearly visible in the response.

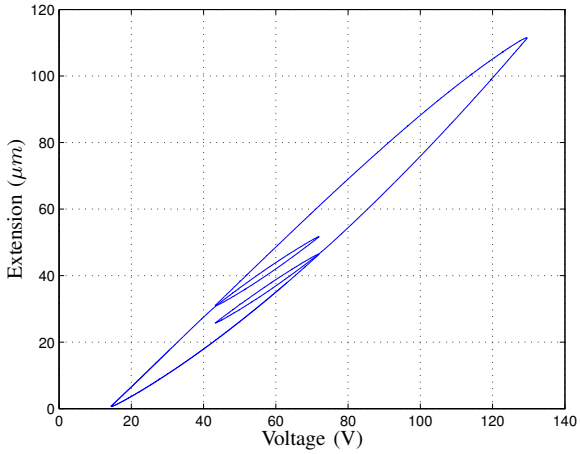

Fig. 3. Extension of the piezo actuator as function of the input for the experiment in Fig. 2. Note the complex behavior of the hysteresis, which exhibits both rate and amplitude dependency.

appears in the frequency range 33–47 Hz in all of the three axes.

The locations of the eigenfrequencies are important since they limit the achievable bandwidth, *i.e.*, the achievable velocity of the control loop, in the final closed-loop control system. Increasing the bandwidth beyond the resonance frequency requires a lot of control actuation and the sensitivity to modeling errors becomes significant.

IV. Modeling of the mechanical construction

In order to design control algorithms, it is advantageous to perform modeling of the HDCM prior to the design. Two different methods for modeling can be chosen. Firstly, modeling based on mechanical relations can be established, where the construction specific parameters are either analytically calculated or experimentally determined.

The other approach is to consider black-box input-output

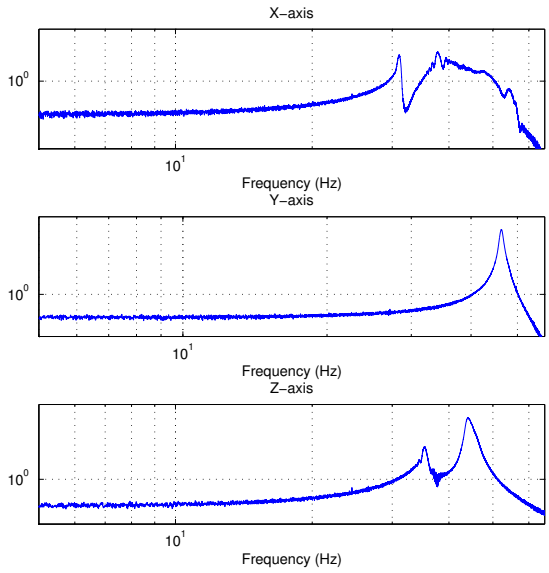

Fig. 4. Estimated frequency spectra in the three Cartesian directions.

models without investigating the internal mechanical construction. This is a common approach in model-based control which results in satisfactory control performance given that the model captures the essential dynamics of the process. This approach is investigated in this paper for modeling of the HDCM.

A. Identification based on black-box models

Using system identification methods [6], mathematical models describing the HDCM can be determined. The axes can be assumed to be decoupled, conditioned that the mechanical design is made such that the motions of the different directions are independent. This assumption is made in this paper. Consequently, each axis is considered as a system with one input and one output. Identification of the models was done in the System Identification Toolbox [7] in MATLAB and the State space Model Identification (SMI) toolbox [8] for identification of state-space models.

Accordingly, consider discrete-time state-space models of the innovation form

$$x_{k+1} = \Phi x_k + \Gamma u_k + v_k \tag{1}$$
$$y_k = C x_k + D u_k + e_k \ , \tag{2}$$

where $u_k \in \mathbb{R}^m$ is the input, $x_k \in \mathbb{R}^n$ is the state vector, $y_k \in \mathbb{R}^p$ is the output and v_k and e_k are noise sequences. The matrices $\{\Phi, \Gamma, C, D\}$ in the state-space representation are then identified using one of the available implementations of sub-space based identification methods, such as the N4SID-method [9] and the MOESP algorithm [10]. During the identification of the models, a Kalman gain vector for a minimum variance estimate of the states in the model is also determined, based on the noise properties.

B. Collection of input-output data

The collection of experimental input-output data is performed in such a way that the input u_k is considered to be a scaled version of the input voltage to the actuator, whereas the output y_k is defined to be the position of the spindle as measured by the capacitive sensor.

When performing system identification, an appropriate input signal has to be chosen, such that the system is excited properly. A common choice is to use a pseudo-random binary signal (PRBS), since it is a broad-spectrum signal. However, in this paper a chirp-signal is chosen—*i.e.*, a sinusoid with constant amplitude and linearly increasing frequency—as input, since this signal gives excitation in a well-defined frequency range. Consequently, the start and end frequency in the chirp-signal have to be chosen based on the frequency range of interest. Given the frequency spectra displayed in Fig. 4, a reasonable range of excitation is 10–60 Hz.

C. Model-order selection and preprocessing of the data

When performing identification of the state-space models, a model order has to be chosen. For this purpose, the singular values calculated during the identification procedure using the N4SID or MOESP algorithms are utilized. By plotting these singular values, the gap between the model and the noise level is identified. Based on this information, a suitable model order can be chosen.

Before the identification procedure is initiated, the input-output data is processed, such that the mean and the linear trend are removed. The input-output data is acquired at a sampling rate of 1000 Hz. Prior to the identification, the data is decimated to a sample rate of 1000/6 $\approx$ 167 Hz. This choice is suitable, given the location of the eigenfrequencies in the different axes.

D. Identified models

Experimentally identified discrete-time state-space models on the form (1)–(2) of the x, y and z-directions in the open-loop system were estimated. All models are of the same format. However, the model orders are different in different directions, reflecting the number of natural eigenfrequencies, *cf.* the frequency spectra in Fig. 4. The model orders are 4, 2 and 5 in the x- y- and z-directions, respectively. The model order selection was based on the singular values analysis during the identification procedure. As an example, the model obtained using the SMI toolbox in the y-direction is

$$x_{k+1} = \begin{bmatrix} -0.1846 & 1.071 \\ -0.8762 & -0.1588 \end{bmatrix} x_k + \begin{bmatrix} -1.029 \\ -0.06196 \end{bmatrix} u_k \tag{3}$$
$$y_k = \begin{bmatrix} -0.4567 & -0.03502 \end{bmatrix} x_k + 0.3321 u_k \ . \tag{4}$$

The frequency spectra of the identified models are shown in Fig. 5. It is noted that there is good correspondence with the estimated periodograms in Fig. 4. The pole-zero plot of the identified models in the x- and y-directions can be seen in Figs. 6–7, *cf.* the Bode magnitude for the corresponding models. A measure of the fit of the models, are the *variance accounted for* (VAF) values. These numbers

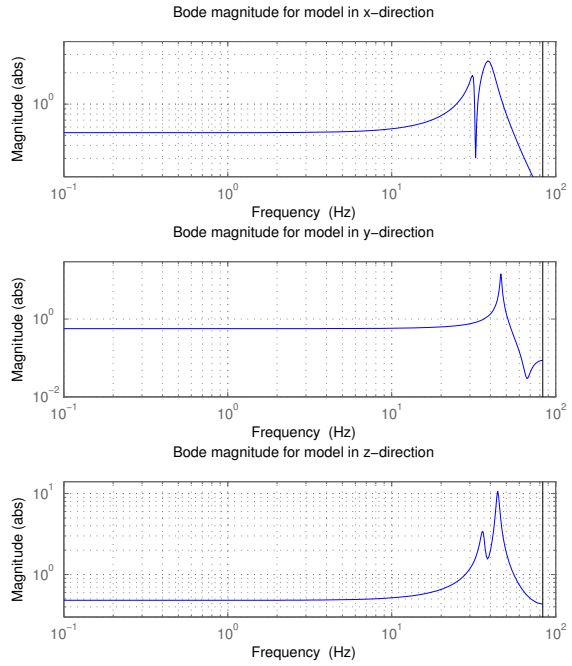

Fig. 5. Bode magnitude of the discrete-time state-space models identified using sub-space identification, in the x- y- and z-directions, respectively.

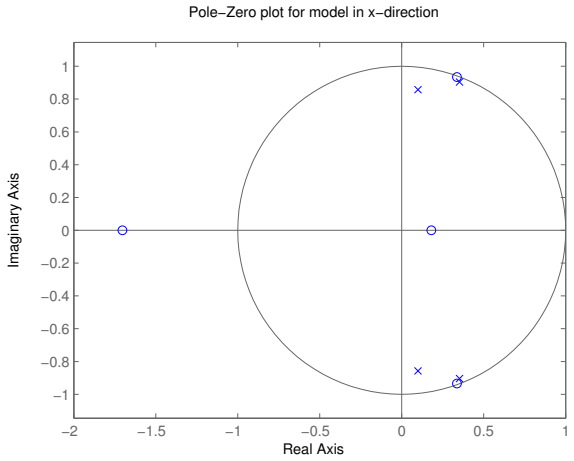

Fig. 6. Pole-zero plot for the identified state-space model in the x-direction.

are 92.5, 99.5 and 97.1 for the identified models in the x-, y- and z-directions, respectively. This indicates that the models capture the essential dynamics of the system.

V. Position control of the HDCM

The control problem of the HDCM can be divided into two parts. Firstly, the nonlinear effects of the piezo actuators need to be reduced. Secondly, the oscillatory mechanical construction needs to be accurately position controlled. The control structure chosen in this paper is described below.

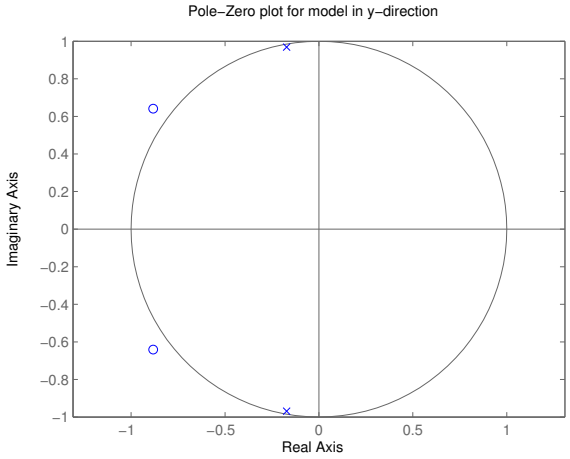

Fig. 7. Pole-zero plot for the identified state-space model in the y-direction.

A. Inner piezo actuator control loop

Nonlinear systems can be controlled by both model-based feedforward control and with feedback control. Several approaches to modeling the hysteresis and subsequent model-based control design have been presented in literature, such as the Prandtl-Ishlinskii model and the Preisach model, *e.g.*, [11], [12], [13]. However, as the extensions of the piezo actuators in the HDCM are available for measurement with the strain gauges, we choose another more straightforward solution, where an inner feedback loop is closed around the nonlinear actuator. The controller is a linear PID controller, whose continuous time transfer function $G_C(s)$ can be written as

$$G_C(s) = K_p + \frac{K_i}{s} + \frac{sK_d}{1 + sK_d/N} \ , \qquad (5)$$

where K_p, K_i and K_d are controller parameters. It is noted that the derivative part in the controller is lowpass filtered, in order to reduce the amplification of high-frequency noise contaminating the measured signal from the strain gauge. The cutoff frequency in the lowpass filter is determined by the parameter N. The PID controller also has to be accompanied by an anti-windup scheme, to handle the case when the controller saturate the actuators. Discretization of this continuous time controller for implementation in the dSPACE system is straightforward, see, *e.g.*, [14].

In order to reduce the nonlinear effects in the piezo actuators, the proportional gain K_p and the integral gain K_i should be increased as much as possible, without causing instability. It will be shown by experimental results in Section VI, that this approach—*i.e.*, using a linear controller for reducing the nonlinear effects in the piezo actuator—results in satisfactory performance of the control of the piezo actuators.

B. Model-based feedback control of the HDCM

By utilizing the identified state-space models, a state feedback control loop can be designed for each of the three Cartesian directions in the HDCM. However, new models

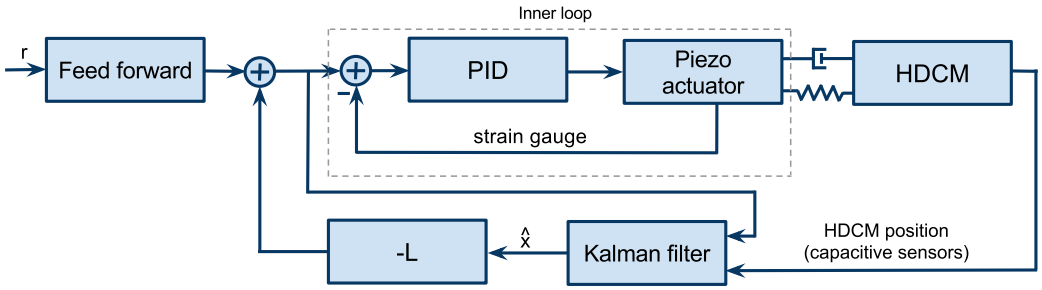

Fig. 8. Control structure for model-based control of the HDCM, where each Cartesian axis is considered separately.

need to be identified after closing the inner feedback loop around the piezo actuators, where the reference signal to the inner PID control loop is considered as the input instead. Since the difference compared to the open loop models presented in the previous Section is small, the models with the closed inner loop are not presented here.

State feedback is an appropriate structure, since damping can be introduced in the construction by suitable control design. The control law for state feedback control of the system (1)–(2) can be stated as follows

$$u_k = -Lx_k + u_{ff} \ , \tag{6}$$

where the parameter vector L is to be chosen and u_{ff} is the feedforward control signal. The design procedure is to determine the L-vector by LQ optimal control [14], *i.e.*, such that the cost function

$$J(u) = \sum_{k=1}^{\infty} x_k^T Q x_k + u_k^T R u_k \ , \tag{7}$$

where the matrices Q and R are user defined weights in the optimization, is minimized.

Since all states in the state-space model of the HDCM are not available for measurement, a Kalman filter is introduced for estimation of the states, based on the measured position signal and the identified model. The Kalman filter is organized as [14]

$$\hat{x}_{k+1} = \Phi \hat{x}_k + \Gamma u_k + K(y_k - C\hat{x}_k - Du_k) \tag{8}$$

$$\hat{y}_k = C\hat{x}_k + Du_k \ , \tag{9}$$

where the estimated states $\hat{x}_k$ and the estimated output $\hat{y}_k$ have been introduced. Since the identified model is based on experimental data, where the mean are subtracted from the real data, a *disturbance state* is added to the observer, *i.e.*, the new constant state

$$\hat{x}^e_{k+1} = \hat{x}^e_k \ , \tag{10}$$

is introduced. By adding this state, the correct static gain for the estimation is achieved [14]. The Kalman gain K is determined by pole placement, *i.e.*, such that the eigenvalues of the matrix $(\Phi - KC)$ are appropriate. The model identification procedure provides the Kalman gain vector for estimation of the states in the model. The corresponding pole placement is used also in the Kalman filter with the disturbance state, but with one additional pole corresponding to the extra disturbance state.

The control law for the state feedback control is then based on the estimated states, *i.e.*, $u_k = -L\hat{x}_k + u_{ff}$. In order to remove stationary errors in the position control loop, integral action is introduced in the state feedback. This is done by extending the state vector with the integral state

$$x_i(t) = \int_0^T (r(t) - y(t)) \ \mathrm{d}t \ , \tag{11}$$

where the reference signal $r(t)$ has been introduced. Note that this state needs to be discretized prior to implementation in the dSPACE system. The feed forward control signal u_{ff} is chosen as a direct term from the reference signal, $u_{ff} = l_r r$. The control structure is summarized in Fig. 8.

VI. Experimental results

Several experiments were performed in order to evaluate the performance of the control design. Firstly, the PID controller for the nonlinear piezo actuator is evaluated.

A. Inner PID control loop

The inner feedback control loops for controlling the extensions of the piezo actuators are closed and the parameters of the controllers are experimentally tuned. The result in the y-direction when applying a triangular wave as reference signal is presented in Fig. 9. It is observed that the control is working satisfactory, despite the nonlinearities in the piezo actuator, and that the control error is approximately ± 1 μm. This shows that the PID controller is a satisfactory control structure, as the precision required in the inner control loop is achieved.

B. Evaluation of the control design

In order to evaluate the model-based control design on the experimental setup, a reference signal, recorded as the deflection of the robot during a milling operation in one dimension, is used. The deflection of the robot was thereby measured with a laser sensor. The recorded signal corresponds to the deflection of the industrial robot in the milling direction, which equals the y-direction of the HDCM.

In order to determine the state feedback vector L, the weight matrices Q and R in the LQ-design need to be determined. Based on the identified model for the HDCM in the y-direction, the characteristics of the closed loop system

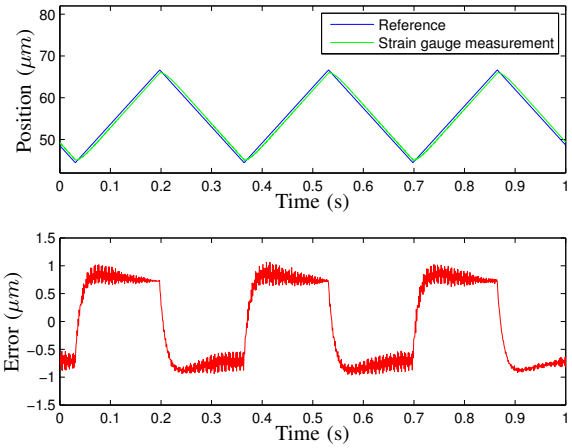

Fig. 9. Performance of the inner PID control loop in the y-direction when applying a 3 Hz triangular wave as input.

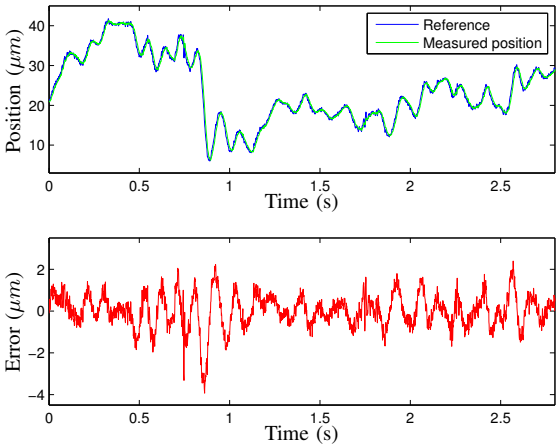

Fig. 11. Control performance in the inner PID control loop in the y-direction.

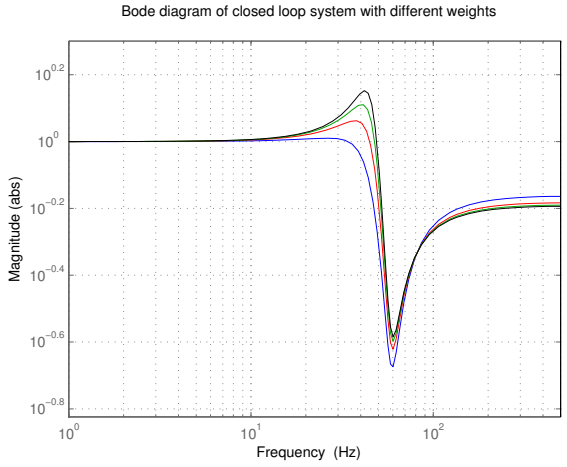

Fig. 10. Bode diagram for the closed loop system for $Q = I$ and different choices of the R-matrix in the LQ-design. The choices of R are 1.0, 2.0, 3.0 and 4.0 for the blue, red, green and black line, respectively.

was investigated for different weight matrices. Especially, the choice of the R-matrix determines the aggressiveness of the controller. Bode plots of the closed loop system for different choices of R, where the Q-matrix has been chosen as the identity matrix, can be seen in Fig. 10. The direct term l_r in the control law has been chosen such that the static gain is one in all cases. It is noted that a lower weight results in a more aggressive controller, where the resonance in the system is well damped, at the cost of reduced bandwidth. Hence, the controller needs to be tuned as a trade-off between the attenuation of the poorly damped resonance in the system and the aggressiveness of the controller. A too aggressive controller may result in unsatisfactory control performance or even instability when applied to the experimental setup, due to noisy measurement signals.

Experiments were performed on the real setup with varying weight matrices. Also, the integral state was added to the state feedback, whose influence is determined by the parameter l_i. The following set of weight matrices

$$Q = \begin{bmatrix} 1 & 0 \\ 0 & 1 \end{bmatrix} \qquad \text{and} \qquad R = 2.5 \tag{12}$$

turned out to result in satisfactory control performance. The reference signal is filtered using a notch filter, where the notch is located at the eigenfrequency of the HDCM in the y-direction, as observed in the frequency spectrum in Fig. 4. This is done in order not to excite the mechanical resonance in the construction. Another option is to lowpass-filter the reference signal. However, since the construction itself is of lowpass-character, frequencies above the natural eigenfrequency in the reference signal will be attenuated.

The recorded signal was applied as reference signal in the y-direction of the HDCM. Fig. 11 shows the control performance of the inner PID controller loop. It is noted that the control error with this reference signal, which contains high frequencies, is within approximately ± 3 μm. Fig. 12 shows the spindle position, as measured by the capacitive sensor. Also this figure indicates good control performance, with a control error of within approximately ± 15 μm.

It is observed in Fig. 12 that the control error signal exhibits periodic behavior of different frequencies. The frequency spectrum of the control error signal is displayed in Fig. 13. Three peaks at 9, 140 and 250 Hz are clearly visible. The first peak corresponds to the eigenfrequency of the robot and the higher frequencies are related to eigenfrequencies of the piezo actuator, the rotation of the spindle and the impact of the milling tool on the workpiece. Further, it is noted that the first significant eigenfrequency of the HDCM in the y-direction at 47 Hz is well damped as a result of the control design.

VII. Conclusions and Future Work

This paper has investigated modeling and control of a piezo-actuated high-dynamic compensation mechanism. Based on an experimental dynamic characterization of the

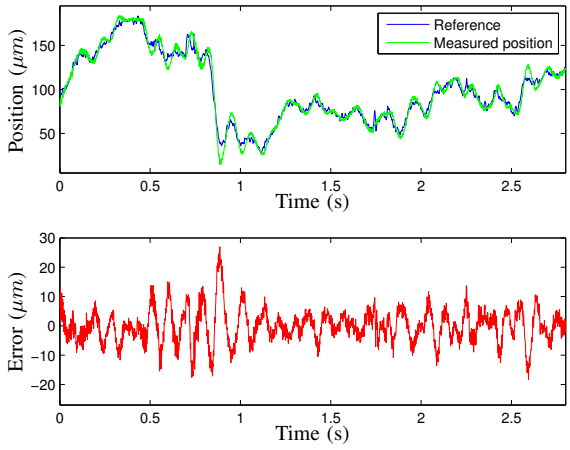

Fig. 12. Performance of the model-based spindle positioning control in the y-direction.

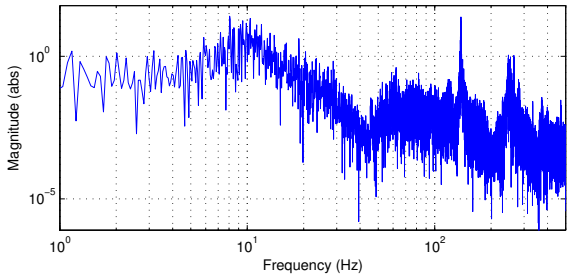

Fig. 13. Spectrum of the control error signal.

mechanical construction and the nonlinear effects in the piezo actuators, black-box models were experimentally identified using system identification methods.

In order to reduce the nonlinear effects in the piezo actuators, a high-gain feedback controller was introduced and turned out to give satisfactory results. Further, based on the identified state-space models, a control scheme utilizing state feedback combined with a Kalman filter for estimation of the states in the model was developed. The control structure was realized in a discrete-time implementation and experimentally verified on the real setup of the HDCM. By tuning the state feedback controller appropriately, damping was introduced in the mechanical construction by control design. The resulting control error for a reference signal recorded during a milling operation was approximately ± 15 μm, which is well below the desired accuracy of 50 μm for the whole milling task.

Based on the experimental results presented in this paper, the model-based approach for control of the HDCM is promising. However, the control scheme needs to be tested further during milling operations in order to take the process-specific disturbances into account in the control scheme. This can be achieved by modeling of the disturbances specific for the milling process, such as the spindle rotation and the forces occurring during milling operations. Including this information in a feedforward control scheme is likely to reduce the remaining errors and make the controller more robust to disturbances.

The HDCM-unit will be equipped with a 3D-accelerometer sensor, and the acceleration signal will be combined with the identified models in order to increase the quality of the estimate of the states, and hence the control performance.

VIII. Acknowledgments

The research leading to these results has received funding from the European Union's seventh framework program (FP7/2007-2013) under grant agreement #258769 (COMET: Plug-and-produce COmponents and METhods for adaptive control of industrial robots enabling cost effective, high precision manufacturing in factories of the future).

The authors want to acknowledge Prof. Karl J. Åström and Dr. Klas Nilsson for valuable advice during the work and Mr. Marius Beul for taking part in the implementation work and laboratory experiments.

References

[1] COMET, 2011, EU/FP7-project: *Plug-and-produce COmponents and METhods for adaptive control of industrial robots enabling cost effective, high precision manufacturing in factories of the future*, URL: http://www.cometproject.eu.

[2] A. Puzik, A. Pott, C. Meyer, and A. Verl, "Industrial robots for machining processes in combination with an additional actuation mechanism for error compensation," in *7th Int. Conf. on Manufacturing Research (ICMR)*, 2009.

[3] A. Puzik, C. Meyer, and A. Verl, "Results of robot machining with additional 3D-piezo-actuation-mechanism for error compensation," in *7th CIRP Int. Conf., Intelligent Computation in Manufacturing Engineering: Innovative and Cognitive Production Technology and Systems*, 2010.

[4] *DS1103 PPC Controller Board—Hardware Installation and Configuration*. Paderborn, Germany: dSPACE GmbH, 2007.

[5] *Real-Time Workshop 7: Users's Guide*. Natick, Massachusetts: The MathWorks, Inc., 1994–2010.

[6] R. Johansson, *System Modeling and Identification*. Englewood Cliffs, New Jersey: Prentice Hall, 1993.

[7] L. Ljung, *System Identification Toolbox 7: Users's Guide*. Natick, Massachusetts: The MathWorks, Inc., 1988–2010.

[8] B. Haverkamp and M. Verhaegen, *SMI Toolbox: State Space Model Identification Software for Multivariable Dynamical Systems*. Delft, The Netherlands: Delft University of Technology, 1997.

[9] P. van Overschee and B. De Moor, "N4SID: Subspace algorithms for the identification of combined deterministic-stochastic systems," *Automatica*, vol. 30, no. 1, pp. 75–93, 1994.

[10] M. Verhaegen and P. Dewilde, "Subspace model identification—The output-error state-space model identification class of algorithms," *Int. Journal of Control*, vol. 56, pp. 1187–1210, 1992.

[11] M. Al Janaideh, Y. Feng, S. Rakheja, C.-Y. Su, and C. Alain Rabbath, "Hysteresis compensation for smart actuators using inverse generalized Prandtl-Ishlinskii model," in *Proc. of the 2009 American Control Conference*, St. Louis, Missouri, June 2009, pp. 307–312.

[12] P. Ge and M. Jouaneh, "Tracking control of a piezoceramic actuator," *IEEE Transactions on Control Systems Technology*, vol. 4, no. 3, pp. 209–216, 1996.

[13] P. Krejci and K. Kuhnen, "Inverse control of systems with hysteresis and creep," in *IEE Proc.–Control Theory and Applications*, vol. 148, no. 3. IEE, 2001, pp. 185–192.

[14] K. J. Åström and B. Wittenmark, *Computer-Controlled Systems*. Englewood Cliffs, New Jersey: Prentice Hall, 1997.